Disorder in Crystalline Organosilicon Compounds Si_2R_6: A Solid-State NMR Study

Jörg Kümmerlen† and Angelika Sebald*,‡

Bayerisches Geoinstitut, Universität Bayreuth, D-95440 Bayreuth, Germany

Received February 18, 1997⊗

Variable-temperature ^{13}C and ^{29}Si CP/MAS NMR studies of the solid-state dynamic properties of compounds Si_2R_6 (R = ^{t}Bu, **1**; R = $SiMe_3$, **2**) are reported. Both structural phase transitions and internal molecular reorientational processes are detected by high-resolution solid-state NMR. Internal reorientational processes in **1** and **2** are not suppressed by massive steric *intra*molecular crowding. Quantification of the internal ^{t}Bu reorientation characteristics in **1**, as determined experimentally by NMR in conjunction with spectral line shape simulations, is in good agreement with the results of molecular dynamics simulations based on the single-crystal structure of **1**.

Introduction

Solid-state NMR has a longstanding tradition in the investigation of dynamic properties of crystalline solids.[1] In the past, such studies have largely been a domain of wide-line NMR techniques and relaxation time measurements, which make accessible a very wide range of temperatures but lack all spectral resolution. Hence, the interpretation of temperature-dependent effects observed in wide-line NMR experiments has to rest on tentative assignments to specific modes of reorientation. Static ^2H NMR studies, in favorable cases, may allow the identification of particular reorientational modes based on their specific influence on the static ^2H line shape.[2] Again, static ^2H studies offer a wide range of accessible temperatures but fully or selectively deuterated samples are necessary. One- and two-dimensional high-resolution solid-state NMR techniques offer the distinct advantage of high spectral resolution, at the expense of a restricted accessible temperature range (under MAS conditions, usually the temperature range $T \approx 130-360$ K is accessible experimentally). High spectral resolution does allow the unique identification and quantification of specific reorientational modes in crystalline solids. In particular, single-crystal X-ray diffraction information, if available, can be exploited advantageously in high resolution solid-state NMR studies. The disadvantage of a restricted accessible temperature range under MAS conditions is at least partially compensated by the possibility of extending the range of observable correlation times by, for instance, two-dimensional exchange spectroscopy.[3]

Many spherically, or nearly spherically shaped, molecular solids display a wealth of dynamic orientational disorder, including phase transitions to the plastically crystalline state before melting.[1,4] An example of a tetrahedral molecule is adamantane,[1] but also homologues of ethane such as hexachloroethane,[5] hexamethylethane,[6] and hexamethyldisilane[7] show different modes of molecular reorientation and phase transitions as a function of temperature which have been extensively investigated by various experimental techniques and molecular dynamics simulations. Here we present a variable-temperature ^{13}C and ^{29}Si CP/MAS NMR study of disorder occurring in two ethane homologues Si_2R_6 (R = ^{t}Bu (**1**), $SiMe_3$ (**2**)). **1** and **2** differ from previously studied solid ethane homologues, as **1** and **2** are characterized by considerable *intra*molecular steric overcrowding.

Results and Discussion

When one considers the structural and dynamic solid-state properties of crystalline molecular compounds Si_2R_6 such as **1**, $Si_2{}^tBu_6$, and **2**, $Si_2(SiMe_3)_6$, different modes of molecular reorientation are to be taken into account, in addition to the possible presence of static structural disorder and structural phase transitions. The various possible reorientational modes for **1** and **2** are illustrated in Chart 1.

Chart 1. Possible Modes of Reorientation in Compounds $Si_2(XMe_3)_6$ (X = C, Si): (a) Internal Me Reorientation; (b) Internal ^{t}Bu (or $SiMe_3$) Reorientation; (c) Internal Reorientation around the Central Si−Si Bond; (d) Whole-Molecule Reorientation around an Arbitrary Axis

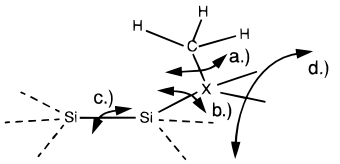

X = Si, C

Assuming that variable-temperature ^{13}C and ^{29}Si CP and CP/MAS techniques are the available solid-state

† E-mail: joku@uni-bayreuth.de.
‡ E-mail: angelika.sebald@uni-bayreuth.de.
⊗ Abstract published in *Advance ACS Abstracts,* June 1, 1997.

(1) Parsonage, N. G.; Staveley, L. A. K. *Disorder in Crystals*; Clarendon Press: Oxford, U.K., 1978.
(2) Schmidt-Rohr, K.; Spiess, H. W. *Multidimensional Solid-State NMR and Polymers*; Academic Press: London, 1994.
(3) Kümmerlen, J.; Sebald, A. In *Encyclopedia of NMR*; Grant, D. M., Harris, R. K., Eds.; Wiley: New York, 1995; pp 4127−4132, and references given therein.
(4) Sherwood, J. N. *The Plastically Crystalline State*; Wiley: Chichester, U.K., 1979.
(5) Criado, A.; Munoz, A. *Mol. Phys.* **1994**, *83*, 815.
(6) Rothwell, W. P.; Waugh, J. S. *J. Chem. Phys.* **1981**, *74*, 2721.
(7) Aksnes, D. W.; Kimtys, L. *Acta Chem. Scand.* **1995**, *49*, 722.

S0276-7333(97)00120-9 CCC: $14.00

NMR tools, all of these reorientational modes except for internal Me reorientation are amenable to investigation. Fast internal Me reorientation would have to be studied by variable-temperature ^{2}H wide-line NMR techniques on fully deuterated compounds. One- and two-dimensional, variable-temperature ^{13}C MAS NMR techniques are suitable to detect and quantify chemical exchange between crystallographically inequivalent methyl sites, brought about by internal ^{t}Bu (**1**) or $SiMe_3$ (**2**) reorientation. The same techniques allow investigation of mutual chemical exchange of the ^{t}Bu and $SiMe_3$ groups, respectively, due to internal reorientation around the central Si−Si bond in **1** and **2**. Overall molecular reorientation, such as isotropic tumbling or reorientation around one (or more) preferred molecular axis, can be identified by variable-temperature ^{29}Si NMR (in addition to its effects on the respective ^{13}C spectra). Note that for **1** and **2** the manifestation of internal SiR_3 reorientation around the central Si−Si bond in ^{13}C and ^{29}Si CP/MAS spectra will be indistinguishable from the effects of reorientation of the entire molecule around an axis coincident with the Si−Si bond direction.

Compounds **1** and **2** represent fairly special circumstances with respect to the various possible modes of internal or overall molecular reorientation in solid compounds Si_2R_6. Despite the long Si−Si central bonds found for both solids (270 pm in **1**[8] 240 pm in **2**[10,11]) the bulky substituents R = ^{t}Bu, $SiMe_3$ still lead to considerable steric strain in the molecular unit. In fact, the steric requirements of the bulky ligands R in **1** and **2** are such that "distributing" six such ligands R over one central Si−Si bond, regardless of a very long Si−Si bond distance, still enforces *intra*molecular mutual R−R contacts considerably shorter than the typical van der Waals (vdW) radii of R = ^{t}Bu, $SiMe_3$.[10,11]

Compound 1, $Si_2{}^tBu_6$. Single-crystal X-ray diffraction at room temperature shows **1** to crystallize in space group *Ibca*, with half a molecule representing the asymmetric unit and with three crystallographically inequivalent ^{t}Bu groups per Si atom.[8,12] Hence, in the absence of disorder effects at room temperature **1** should yield one resonance in ^{29}Si CP/MAS spectra (with a ^{29}Si shielding tensor close to axial symmetry); in the ^{13}C CP/MAS spectra of **1** we should expect three ^{13}C resonances for the quaternary carbons and nine ^{13}C resonances for the nine crystallographically inequivalent methyl groups. ^{29}Si CP/MAS spectra (59.6 MHz) at T = 293 K display one sharp ^{29}Si resonance for **1** ($\delta(^{29}Si)$ 33.5 ppm); ^{13}C CP/MAS spectra (75 MHz) at T = 293 K show one slightly broadened resonance for the quaternary carbon atoms ($\delta(^{13}C)$ 28.0 ppm) and a strongly broadened resonance for the methyl carbon atoms centered at $\delta(^{13}C) \sim 35.4$ ppm. These chemical shift ranges are very similar to the isotropic ^{13}C and ^{29}Si chemical shifts reported for **1** in C_6D_6 solution at ambient temperature.[8]

Figure 1 shows 75 MHz ^{13}C CP/MAS spectra of **1** as a function of temperature, only in the temperature range of ca. 180−205 K the multiplicity of the methyl ^{13}C resonances is resolved, as predicted from room-temperature single-crystal X-ray diffraction. The three ^{13}C resonances of the three inequivalent quaternary carbon atoms in the Si^{t}Bu$_3$ unit are resolved in the temperature range $T \approx 180-240$ K. Below T = 180 K, further broadening of all ^{13}C resonances is observed.

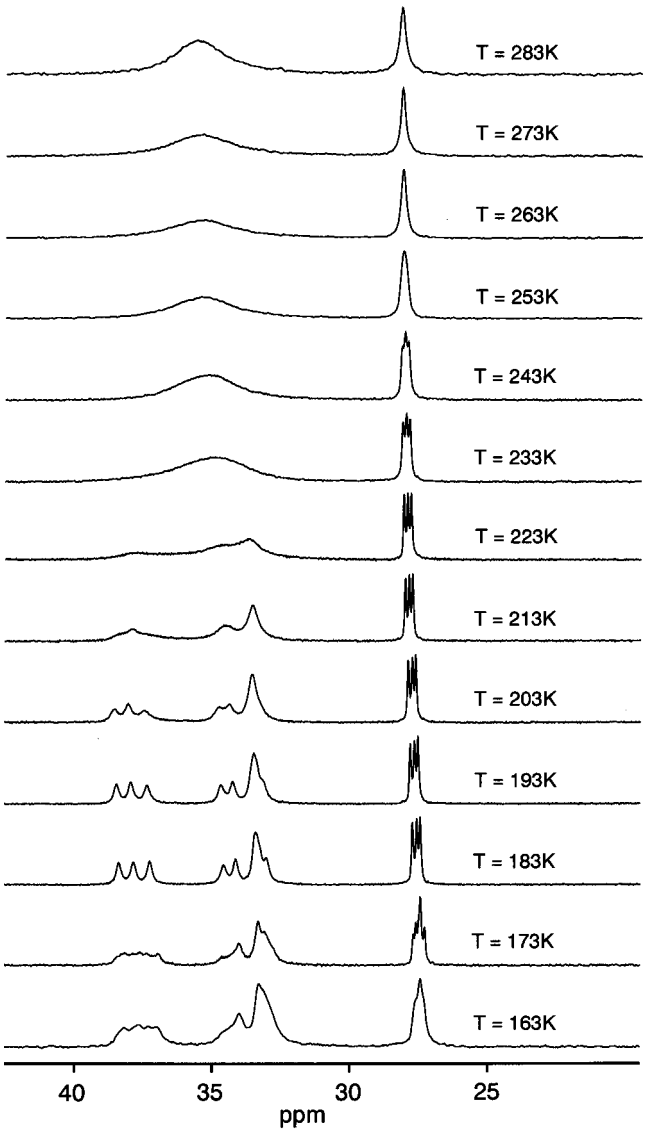

Figure 1. ^{13}C CP/MAS spectra ($\omega_0/2\pi$ = 75 MHz) of **1** in the temperature range T = 163−283 K.

The interpretation of the temperature-dependent effects in the ^{13}C CP/MAS spectra of **1** is as follows: (i) below T = 180 K we observe the onset of a structural phase transition to an ordered phase of lower symmetry, or of substantially increased static disorder; (ii) in the temperature range T = 180−260 K two different modes of reorientation are active, internal reorientation of the ^{t}Bu groups *and* reorientation around the Si−Si bond axis; (iii) both processes have low activation barriers E_a. In the following we will discuss the rationale for this interpretation, on the basis of experimental ^{13}C and ^{29}Si CP/MAS data of **1** obtained at different magnetic field strengths B_0 = 2.3, 7, and 11 T, on molecular dynamics simulations, and on simulations of ^{13}C CP/MAS spectra in the exchange-broadened regime.

First, we will briefly address the temperature range below T = 180 K. The maximum possible number of ^{13}C resonances consistent with the symmetry requirements of the room-temperature single-crystal X-ray

(8) Wiberg, N.; Schuster, H.; Simon, A.; Peters, K. *Angew. Chem.* **1986**, *98*, 100.
(9) Mallela, S. P.; Bernal, I.; Geanangel, R. A. *Inorg. Chem.* **1992**, *31*, 1626.
(10) Fronczek, F. R.; Lickiss, P. D. *Acta Crystallogr.* **1993**, *C49*, 331.
(11) Bock, H.; Meuret, J.; Ruppert, K. *J. Organomet. Chem.* **1993**, *445*, 19.
(12) Simon, A. Personal communication.

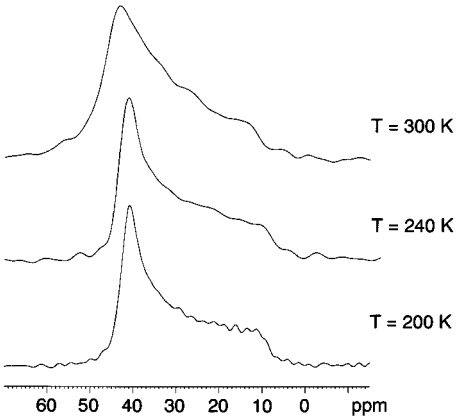

Figure 2. Variable-temperature static ^{29}Si CP spectra of **1** ($\omega_0/2\pi = 59.6$ MHz).

structure of **1** is more or less completely resolved in ^{13}C CP/MAS spectra in the temperature range $T \approx 180-190$ K. Below this temperature region, line shape changes occur in the ^{13}C CP/MAS spectra, characteristic for an increase in the number of (incompletely) resolved resonances, both in the methyl-^{13}C and in the quaternary-^{13}C region. This spectral line shape change occurs at the same temperature at different external magnetic field strengths (see Figures 1 and 3). An increase in the number of resonances beyond the maximum possible number in accord with the room-temperature single-crystal X-ray structure can only be explained by a structural phase transition at $T \approx 180-170$ K to an ordered phase of lower symmetry or by a considerable increase in static disorder at that temperature. From NMR alone we cannot further elucidate the precise nature of this symmetry-lowering process at lower temperatures, and here we will not further discuss the low-temperature structural properties of **1**.

Variable-temperature ^{29}Si static and CP/MAS spectra of **1** also yield useful information concerning higher temperatures. Over the entire temperature range $T = 180-290$ K, one sharp ^{29}Si resonance (with a small temperature-dependent shift of 0.03 ppm K^{-1} toward deshielding for increasing temperature) is observed. This is consistent with the presence of dynamic disorder, both internal ^{t}Bu reorientation and reorientation around the Si−Si axis. Static ^{29}Si CP spectra in the temperature range $T = 200-260$ K exclude the possibility of fast isotropic tumbling of the entire molecule of **1**, as this would lead to vanishing ^{29}Si shielding anisotropy with increasing temperature. We observe (within experimental error) an axially symmetric ^{29}Si shielding tensor for **1** ($\sigma_\perp = 41.0$ ppm, $\sigma_\parallel = 8.0$ ppm), the shape of which is independent of temperature within the range $T = 200-240$ K (see Figure 2). These static ^{29}Si CP spectra are also consistent with the presence of both aforementioned reorientational processes in solid **1**. Only at temperatures $T \geq 290$ K does the shape of the static ^{29}Si shielding tensor also become affected, indicating the onset of further reorientational modes of the entire molecule around axes other than only the Si−Si bond direction.[15] Also the high-temperature regime for solid **1** will not be discussed further; here we will concentrate on the temperature range $T \approx 180-260$ K.

Next, we return to the 75 MHz ^{13}C CP/MAS spectra of **1** depicted in Figure 1. Inspection of these variable-temperature spectra immediately reveals that there must be two different reorientational modes present: one process which renders equivalent the resonances of the three crystallographically inequivalent quaternary carbon atoms and one process which leads to coalescence of the entire methyl region in the spectra. If only one reorientational mode is responsible for both types of coalescence, then any exchange rate affecting the broad range of methyl-^{13}C resonances (from 33.5 to 38.0 ppm in the slow-exchange limit at $T = 183$ K) and leading to their coalescence would correspond to a fast-exchange limit for the much more narrowly spaced quaternary carbon ^{13}C resonances and we would never be able to see the crystallographic splitting of these three resonances (27.6, 27.4, 27.2 ppm at $T = 183$ K). For the moment, we postpone the discussion of the precise nature of these two reorientational processes and consider 125 and 25 MHz variable-temperature ^{13}C CP/MAS spectra of **1** (see Figure 3), in comparison to the 75 MHz ^{13}C CP/MAS spectra shown in Figure 1. In principle, for a given dynamic process the temperature where coalescence is reached is higher for higher external magnetic field strengths. However, the *difference* in coalescence temperature for two different external magnetic field strengths A and B also depends on the activation energy E_a of the process; if coalescence at fields A and B is described by

$$\Delta\nu_A = \nu_0 \exp\left\{-\frac{E_a}{RT_A}\right\}$$
$$\Delta\nu_B = \nu_0 \exp\left\{-\frac{E_a}{RT_B}\right\} \quad (1)$$

respectively (that is assuming, in addition, that E_a is independent of temperature), then

$$\frac{\Delta\nu_A}{\Delta\nu_B} = \frac{\nu_0 \exp\left\{-\frac{E_a}{RT_A}\right\}}{\nu_0 \exp\left\{-\frac{E_a}{RT_B}\right\}} \quad (2)$$

From eqs 1 and 2 one can calculate that for a process with a low activation barrier E_a, we will find smaller differences in coalescence temperature for fields A and B than for a process with a high activation barrier. For instance, an estimation of differences in coalescence temperature for a range of activation energies E_a, using data appropriate to describe coalescence of the methyl-^{13}C region in our 25 (A), 75 (B), and 125 (C) MHz CP/MAS spectra (corresponding to $\Delta\nu_A \approx 130$ Hz, $\Delta\nu_B \approx 390$ Hz, $\Delta\nu_C \approx 650$ Hz, respectively), yields the following calculated differences ΔT in coalescence temperatures for the three different magnetic field strengths: for $E_a = 60$ kJ mol^{-1}, $\Delta T_{AB} = 120$ K and $\Delta T_{AC} = 190$ K; for $E_a = 30$ kJ mol^{-1}, $\Delta T_{AB} = 60$ K and $\Delta T_{AC} = 90$ K; for $E_a = 10$ kJ mol^{-1}, $\Delta T_{AB} = 22$ K and $\Delta T_{AC} = 30$ K. Inspection of the variable-temperature ^{13}C CP/MAS spectra of **1** in Figures 1 and 3 reveals only minor differences with respect to coalescence regimes of the methyl-^{13}C region at the three different magnetic field strengths. Hence, whatever the dynamic process causing coalescence of the methyl-^{13}C resonances in **1**, it must have a low activation barrier E_a. Similar qualitative considerations apply with respect to the coalescence of the ^{13}C resonances of the quaternary carbon atoms.

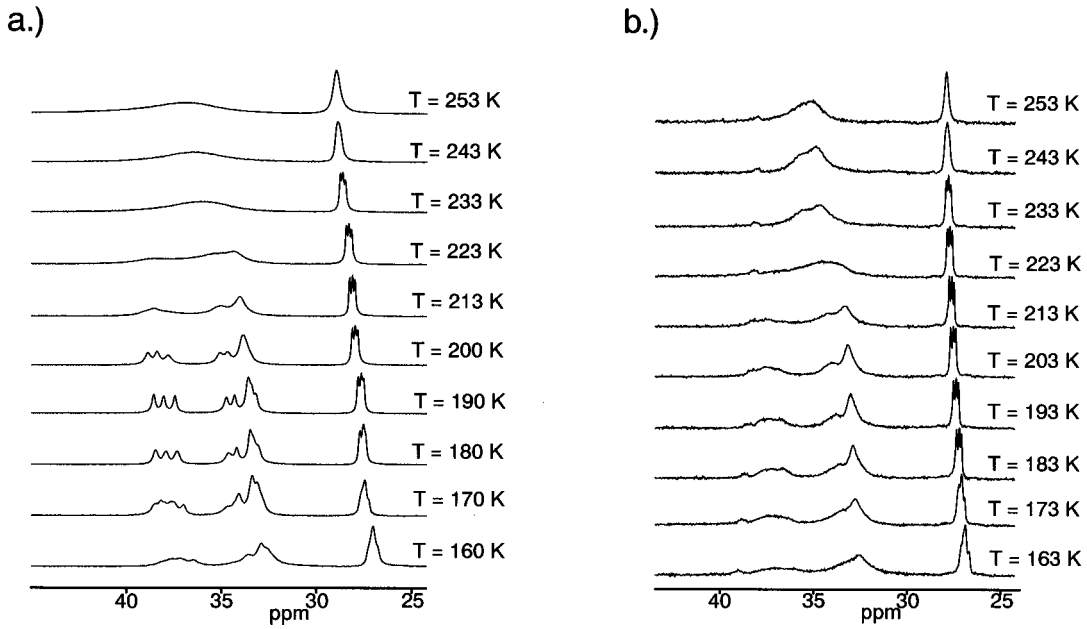

Figure 3. Variable-temperature ^{13}C CP/MAS spectra of **1** at different Larmor frequencies: (a) $\omega_0/2\pi = 125$ MHz; (b) $\omega_0/2\pi = 25$ MHz.

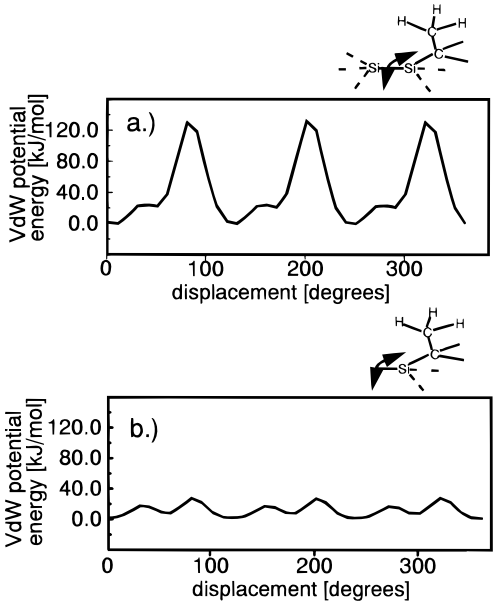

Figure 4. van der Waals potential energy profiles for Si^{t}Bu$_3$ reorientation in **1**: (a) vdW profile in the force field of all atoms (equivalent to a noncooperative, rigid environment); (b) vdW profile in the force field of only the surrounding molecules in the structure.

Further independent information concerning activation barriers of the possible reorientational modes may be obtained from molecular dynamics simulations, based on the room-temperature single-crystal X-ray structure of **1**. van der Waals (vdW) potential energy profiles for the various possible different reorientational modes are obtained by calculating the respective fragment energy as a function of displacement from the crystallographic equilibrium position. Possible reorientational modes leading to coalescence of the three quaternary-^{13}C resonances are either internal reorientation of the ^{t}Bu$_3$Si groups around the Si−Si bond or reorientation of the entire molecule around an axis coincident with the Si−Si bond direction. Figure 4a shows the resulting vdW potential energy profile for internal Si^{t}Bu$_3$ reorientation in the force field of all atoms, assuming a noncooperative, rigid neighboring Si^{t}Bu$_3$ group in the molecule. With a view to the considerable "gearing" of the two bulky R$_3$Si groups in **1**, not surprisingly a very high activation barrier is calculated for this process. Releasing this *intra*molecular steric hindrance by calculating the Si^{t}Bu$_3$ fragment energy of only half a molecule (which can be viewed as equivalent to the fragment energy in the force field of only the surrounding molecules in the structure and, hence, describes the conditions for reorientation of the entire molecule around the Si−Si axis) yields a considerable drop in the height of the respective activation barrier, as is illustrated in Figure 4b. Note a $\pi/3$ dependence of the vdW potential energy profile for this Si^{t}Bu$_3$ reorientational mode. From these calculations we conclude that a feasible reorientational mode of solid **1**, which renders equivalent the three quaternary-^{13}C resonances *and* is of sufficiently low activation energy to be consistent with our experimental ^{13}C CP/MAS observations, might be reorientation of the entire molecule around an axis coincident with the Si−Si bond direction.

Even though, in principle, reorientation around the Si−Si axis—when it takes place at a sufficiently fast rate—could eventually also lead to coalescence in the methyl-^{13}C region, we have to consider a second reorientational process: as explained above, it is not possible to interpret the variable-temperature ^{13}C CP/MAS spectra of **1** in terms of only one dynamic process. We already know that only a process of fairly low activation energy will be consistent with our experimental NMR data. Calculation of the vdW potential energy profiles for internal ^{t}Bu reorientation under different limiting conditions is illustrated in Figure 5.

As is to be expected, internal ^{t}Bu reorientation in the force field of all atoms, i.e. taking only one reorienting ^{t}Bu group in the molecule while keeping all other ^{t}Bu groups stationary, leads to a high activation barrier for this process (see Figure 5a). Removing the effects of *intra*molecular mutual Si^{t}Bu$_3$ hindrance on the internal ^{t}Bu reorientation by calculating the vdW potential

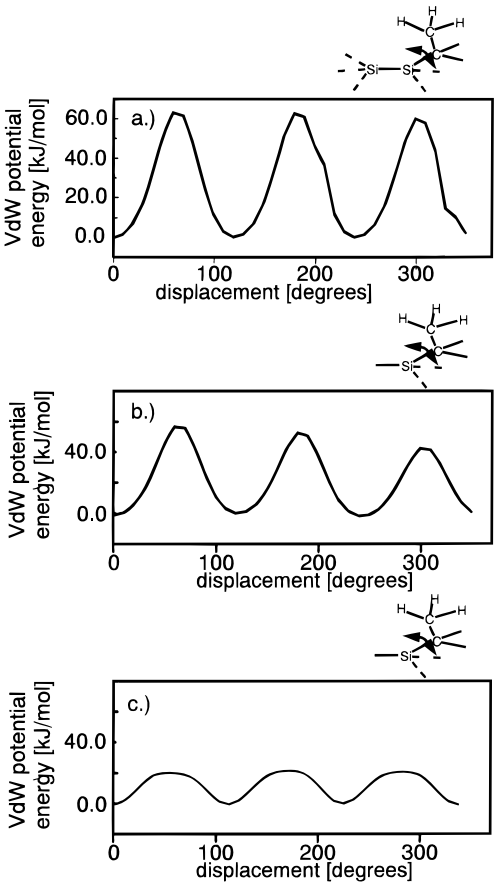

Figure 5. van der Waals potential energy profiles for internal ^{t}Bu reorientation in **1**: (a) vdW profile in the force field of all atoms; (b) vdW profile in the force field of only two further *intra*-Si^{t}Bu groups; (c) vdW profile for internal ^{t}Bu reorientation with allowance for displacement from the crystallographic equilibrium positions for the two remaining ^{t}Bu groups in the Si^{t}Bu$_3$ unit.

energy profile for only half a molecule with one ^{t}Bu group reorienting and the other two ^{t}Bu groups kept in their respective crystallographic equilibrium positions essentially yields an identically high activation barrier (see Figure 5b). Obviously, the height of the barrier of internal ^{t}Bu reorientation is dominated by *intra*-Si^{t}Bu$_3$-group steric hindrance. Allowing for displacement from the crystallographic equilibrium positions for two ^{t}Bu groups while reorienting the third ^{t}Bu group within the Si^{t}Bu$_3$ unit substantially reduces the height of the activation barrier for internal ^{t}Bu reorientation in **1** (see Figure 5c): there is a reduction to about 30% of the value for noncooperative internal ^{t}Bu reorientation. Correlated internal ^{t}Bu reorientation in compounds ^{t}Bu$_3$MX with M = C, Si and X = H, Cl, Br, I has previously been observed in low-temperature solution-state ^{1}H and ^{13}C NMR studies[13,14] and has also been confirmed by molecular dynamics simulations. For ^{t}Bu$_3$SiH in solution, the activation barrier for this process $E_a \approx 25$ kJ mol^{-1} has been calculated and also been determined experimentally.[14] Of course, a cooperative mechanism of simultaneous SiR$_3$ reorientation would also account for a significant reduction in the activation barrier for internal Si^{t}Bu$_3$ reorientation. Unfortunately, our molecular dynamics simulations are not sufficiently accurate to significantly distinguish between internal Si^{t}Bu$_3$ reorientation and whole-molecule reorientation around the Si−Si axis as the preferred low-activation-energy reorientational path. Since these two mechanisms also cannot be distinguished from their effects on the variable-temperature NMR spectra, this question has to remain open. Still, molecular dynamics simulations strongly suggest that the two reorientational models observed in the variable-temperature ^{13}C CP/MAS spectra of **1** are (i) simultaneous internal ^{t}Bu reorientation and (ii) one of the two possible reorientational modes around the Si−Si bond direction. Given the empirical nature of these force field calculations and the approximations made (see Experimental Section), we should stress that these simulations should not be overinterpreted but should rather be considered as representing semiquantitative trends. Nevertheless, these simulations are helpful additional information in identifying the most likely dynamic processes and also independently confirm the qualitative conclusions drawn (low activation barriers E_a) from variable-temperature ^{13}C CP/MAS at different external magnetic field strengths.

Having identified the two reorientational modes in solid **1** causing the temperature-dependent effects in the ^{13}C CP/MAS spectra, there is one last hurdle to pass before we may attempt to quantify our experimental ^{13}C CP/MAS data by means of spectral line shape simulations in the exchange-broadened regime of the methyl-^{13}C region: assignment of the nine methyl-^{13}C resonances in groups of three, representing one ^{t}Bu group each. The most obvious method to obtain this connectivity pattern, in addition to obtaining model-free exchange rates, would be to perform two-dimensional ^{13}C exchange spectroscopy (EXSY)[3] in the slow-exchange regime at $T \approx 185$ K. As it turns out, ^{13}C EXSY is impossible to perform: for all methyl-^{13}C resonances in **1** the longitudinal relaxation times T_1 are extremely short (on the order of 200 ms). These unusually short ^{13}C T_1 relaxation times prevent the use of two-dimensional ^{13}C exchange experiments, even for short mixing times τ_m. Such short relaxation times T_1 for methyl-^{13}C resonances in ^{t}Bu groups are not unique to solid **1**. We have also observed similarly short T_1 relaxation times for the methyl-^{13}C resonances in e.g. solid Pb$_2$(^{t}Bu)$_6$ or (^{t}Bu$_3$Sn)$_2$O.[5] In fact, these short T_1 relaxation times in ^{t}Bu$_3$M moieties may indicate hindrance of the internal Me reorientation in such sterically overcrowded fragments; this aspect has not yet been investigated more closely.

Without the possibility of employing two-dimensional ^{13}C EXSY for assignment and quantification purposes, alternative ways of assigning the nine methyl-^{13}C resonances into groups of three are necessary. Useful qualitative hints can be extracted from considering an idealized conformational environment of the three Me groups in each ^{t}Bu group in the absence of internal ^{t}Bu reorientation, as is shown in Chart 2.

For each of the three ^{t}Bu groups in the Si^{t}Bu$_3$ unit there exists one "unique" Me environment, anti to the second Si^{t}Bu$_3$ unit in the molecule. Low-temperature solution-state ^{13}C NMR on ^{t}Bu$_3$SiH[14] has shown a ^{13}C chemical shift difference of 5.9 ppm between the ^{13}C

(13) Weidenbruch, M.; Flott, H.; Fleischhauer, J.; Schleker, W. *Chem. Ber.* **1982**, *115*, 3444.
(14) Hounshell, W. D.; Iroff, L. D.; Wroczynski, R. J.; Mislow, K. *J. Am. Chem. Soc.* **1978**, *100*, 5212.
(15) Kümmerlen, J.; Sebald, A. Unpublished results.

Chart 2. Newman Projection for an Individual ^{t}Bu Group in 1: View along the Si−Quaternary Carbon Bond Direction, Representing an Idealized Slow-Exchange Regime Conformation

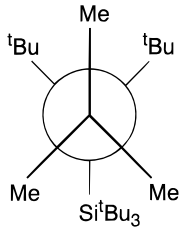

resonance of the unique methyl group and the resonance of the remaining two methyl groups in the ^{t}Bu unit. Around $T = 190$ K we find for solid **1** three resolved, deshielded ^{13}C resonances in a relative 1:1:1 intensity ratio. These three resonances account for roughly one-third of the entire integrated intensity of all nine methyl-^{13}C resonances. The shift difference between the two groups of methyl-^{13}C resonances in an overall 1 (deshielded region):2 (more shielded region) intensity ratio is approximately 4 ppm, in fair agreement with the solution-state ^{13}C NMR results on ^{t}Bu$_3$SiH.[14] Hence, it seems reasonable to assume that the three most deshielded methyl-^{13}C resonances found for solid **1** at $T = 190$ K have to be assigned as representing one Me group in each of the three crystallographically inequivalent ^{t}Bu groups in the Si^{t}Bu$_3$ unit of **1**. This tentative assignment also immediately explains the observation of coalescence over the entire broad range of methyl-^{13}C resonances: if this assignment is correct, then necessarily the remaining two Me groups in each ^{t}Bu group have to belong to the more shielded, incompletely resolved methyl region, and internal ^{t}Bu reorientation will automatically lead to coalescence over the entire methyl-^{13}C region. Similarly, qualitative considerations exclude all assignments which would group together three methyl-^{13}C resonances as representing one ^{t}Bu group solely in the more shielded region: only assignment permutations where every ^{t}Bu group is represented by methyl-^{13}C resonances in the entire range of methyl-^{13}C resonances are in accord with experimental observation.

Despite this qualitative "preselection" many permutations of assignment into groups of three methyl-^{13}C resonances per ^{t}Bu group remain possible. In order to select the correct assignment and to be able to extract activation parameters from simulations/fitting of the variable-temperature one-dimensional ^{13}C CP/MAS spectra of **1**, it is not possible to avoid a fairly tedious, iterative procedure: all remaining possible permutations of assignment have to be simulated, each as a sum of the three respective internal ^{t}Bu reorientational processes within the Si^{t}Bu$_3$ group, and compared to the experimental variable-temperature spectra. In a first selection loop, an initial guess of equal rates of internal ^{t}Bu reorientation of all three independent ^{t}Bu groups has been assumed for the simulation of the corresponding variable-temperature ^{13}C CP/MAS spectra. Among all the possible models of assignment, a large number of permutations is then found to be in considerable disagreement with the overall appearance of the experimental coalescence pattern, while a smaller number of permutations reproduce the overall coalescence pattern reasonably well. Two assignment permutations which yield relatively poor agreement with the overall coalescence pattern and one assignment permutation producing much better agreement with the experimental data are illustrated in Figure 6.

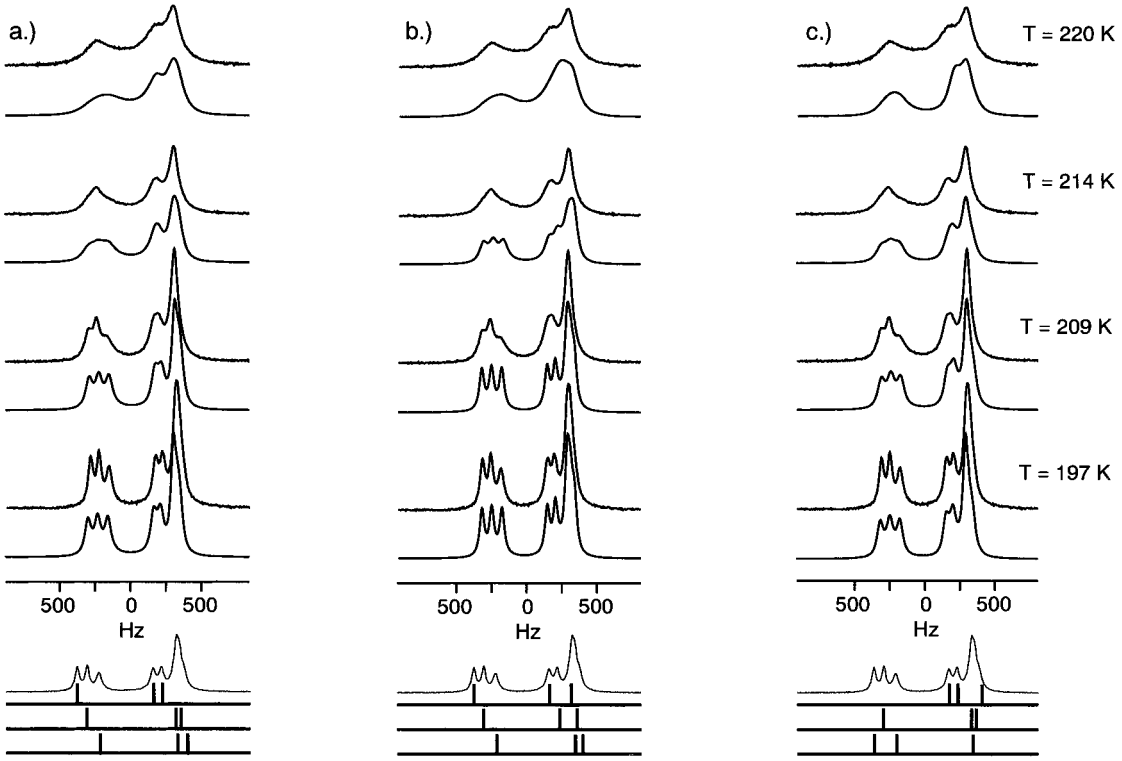

Figure 6. Three different models of assignment within the initial assumption of equal rates for all three three-site exchanges in **1**. Assignments are indicated by the bar codes at the bottom, where equal widths of the bars symbolize equal exchange rates. At the top are shown some representative simulated spectra in comparison to the experimental 125 MHz ^{13}C CP/MAS spectra; only the methyl region is shown, and the respective temperatures are given.

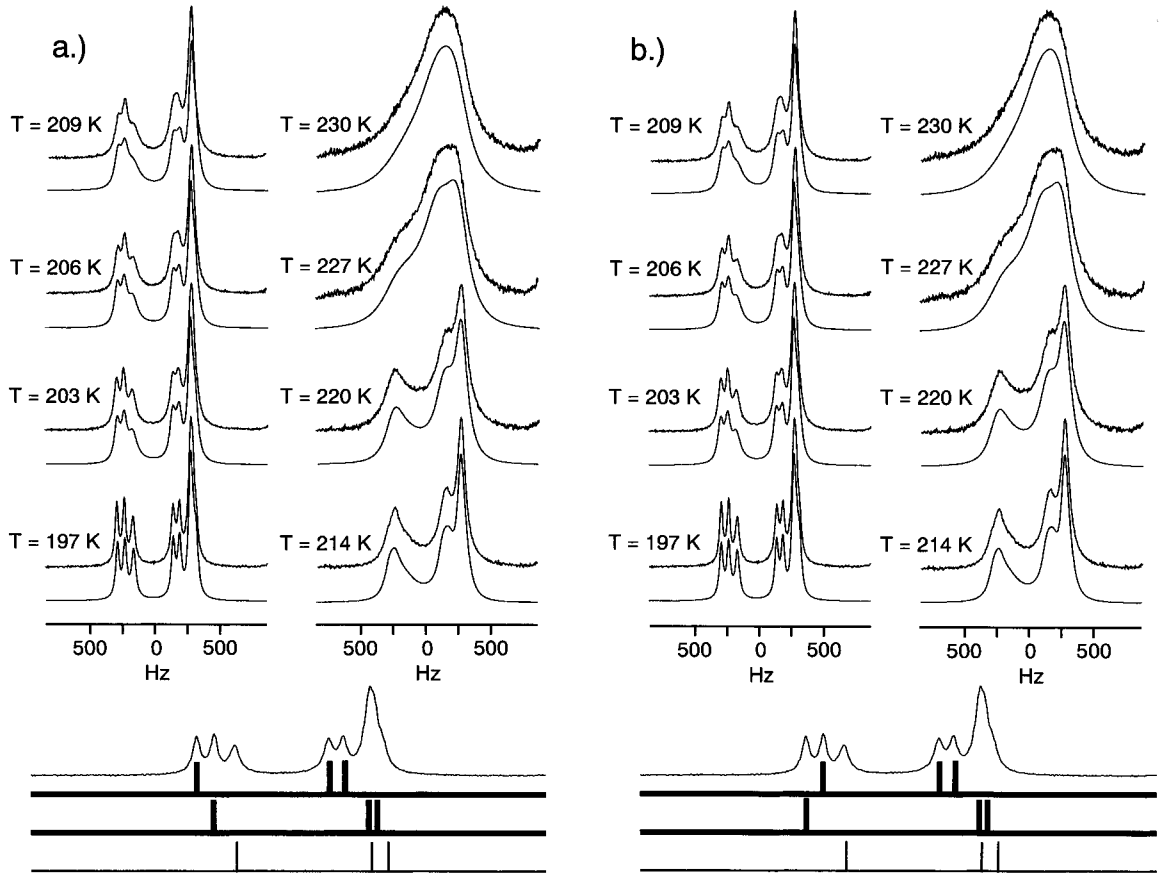

Figure 7. The two final, best models of assignment and unequal exchange rates for internal ^{t}Bu reorientation in **1**. Assignment is indicated at the bottom by bar codes, and narrow widths of the bars indicate faster exchange (twice as fast as the other two ^{t}Bu groups) for the respective ^{t}Bu group. Experimental 125 MHz ^{13}C CP/MAS spectra of **1** are compared to the respective fitted spectra. Only the methyl region is shown, and temperatures are indicated.

While both models b and c, shown as examples in Figure 6, only poorly reproduce even general trends, model a reproduces the overall trends much better, but there are also distinct discrepancies between calculated and experimental spectra with respect to more subtle features of the line shapes. From the assignment model shown in Figure 6a, however, we learn that it is essential to assign the two ^{13}C resonances at 34.2 and 33.8 ppm as belonging to the same ^{t}Bu group; only models with this assignment feature can reproduce the temperature-dependent effects in this spectral region. Further, all models capable of reasonably reproducing the overall trends as a function of temperature have one property in common: all these models deviate from the experimental data in such a way that no further improvement in agreement between calculated and experimental spectra can be reached within this initial-guess assumption of equal internal reorientation rates of all three independent ^{t}Bu groups in the Si^{t}Bu$_3$ unit.

Hence, more refined simulations of the ^{13}C CP/MAS spectra of **1** must allow for the possibility of unequal rates of internal ^{t}Bu reorientation. Note that this requirement is not in contradiction to the findings from the molecular dynamics simulations, where simultaneous internal reorientation of all three ^{t}Bu groups in the Si^{t}Bu$_3$ unit is found to be energetically far more favorable than would be internal ^{t}Bu reorientation in a completely rigid environment: the three ^{t}Bu groups in the Si^{t}Bu$_3$ unit in solid **1** are crystallographically independent and, hence, do not necessarily have to reorient at equal rates. Allowing for unequal reorientation rates immediately leads to considerable improvement in agreement between experimental and calculated spectra for some models of assignment, while disagreement remains for many other assignment permutations. The iterative selection procedure converges towards a model where two ^{t}Bu groups are reorienting at a slower rate than does the third ^{t}Bu group in the Si^{t}Bu$_3$ moiety. By far the smallest final error is found for the two reorientational/assignment permutations shown in Figure 7. The two models shown in Figure 7 cannot be distinguished, as identical final errors are found, and in fact, the two final "best models" for internal ^{t}Bu reorientation in solid **1** are very similar in all other respects as well.

Finally, we have to return to the question of the height of the energy barrier for internal ^{t}Bu reorientation in solid **1**. The barrier height derived from force field calculations based on the room-temperature crystal structure amounts to ca. 20 kJ mol^{-1} for the mechanism of simultaneous reorientation of all three independent ^{t}Bu groups. A plot of reorientation rates as a function of temperature, derived from simulation of the variable temperature 125 MHz ^{13}C CP/MAS spectra for one of the two best models (see Figure 7), is depicted in Figure 8.

The plot in Figure 8 clearly shows a deviation from Arrhenius-type behavior over the (NMR) experimentally accessible temperature range $T = 194-230$ K. In other words, the height of the activation barrier for internal ^{t}Bu reorientation in solid **1** is dependent on temperature. If, for the moment, we ignore this non-Arrhenius

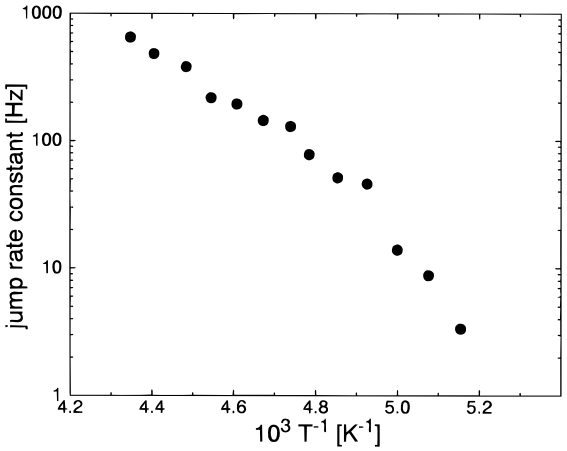

Figure 8. Exchange rates for internal ^{t}Bu reorientation in **1** as a function of temperature, as obtained for model a in Figure 7 from spectral line shape simulation.

behavior over the entire temperature range and only take into account the reorientation rates found in the temperature range $T = 223-230$ K (that is, assuming independence of E_a on temperature over such a small temperature interval), we may derive an estimate of $E_a \approx 25$ kJ mol^{-1} from the slope of the plot near $T = 230$ K. Given the general trend of decreasing E_a with increasing temperature, and taking into account the difference in temperature of ca. 60 K between the highest informative "NMR temperature" of ca. 230 K and the results of the molecular dynamics simulations based on the crystal structure at ambient temperature, the agreement between calculated (molecular dynamics simulations) and experimentally determined (NMR) heights of the activation barrier is surprisingly good. Furthermore, variable-temperature powder X-ray diffraction measurements on **1** indicate a slightly anisotropic shrinking of the unit cell for decreasing temperatures[12] and thus independently support the NMR result of non-Arrhenius behavior of thermally activated internal ^{t}Bu reorientation in solid **1**. Intuitively less surprising is the finding of virtually identical activation barriers for internal ^{t}Bu reorientation in solid **1** and for ^{t}Bu$_3$SiH in solution:[14] in both cases the dominating mechanism is *intra*molecular steric hindrance.

Compound 2, $Si_2(SiMe_3)_6$. The single-crystal X-ray structure of **2** at ambient temperature has been determined;[9-11] **2** crystallizes in space group $R\bar{3}c$. There is half a molecule in the asymmetric unit, and the central Si atom resides on a site of 3-fold symmetry: the three Si atoms of the three $SiMe_3$ ligands are crystallographically equivalent, while the three Me groups per $SiMe_3$ ligand are crystallographically inequivalent. ^{13}C CP/MAS spectra of **2** in the temperature range $T = 273-143$ K are shown in Figure 9.

For temperatures higher than $T \approx 240$ K, only one sharp ^{13}C resonance is observed for the three crystallographically independent methyl groups in **2**, implying that over this temperature range internal $SiMe_3$ reorientation is always fast on the one-dimensional ^{13}C time scale. Before this internal $SiMe_3$ reorientation becomes sufficiently slow to allow detection of the crystallographic splitting (and, hence, to allow extraction of kinetic parameters from simulation of variable-temperature ^{13}C CP/MAS spectra), a structural phase transition to a low-temperature phase of much lower symmetry occurs. This phase transition is also observed

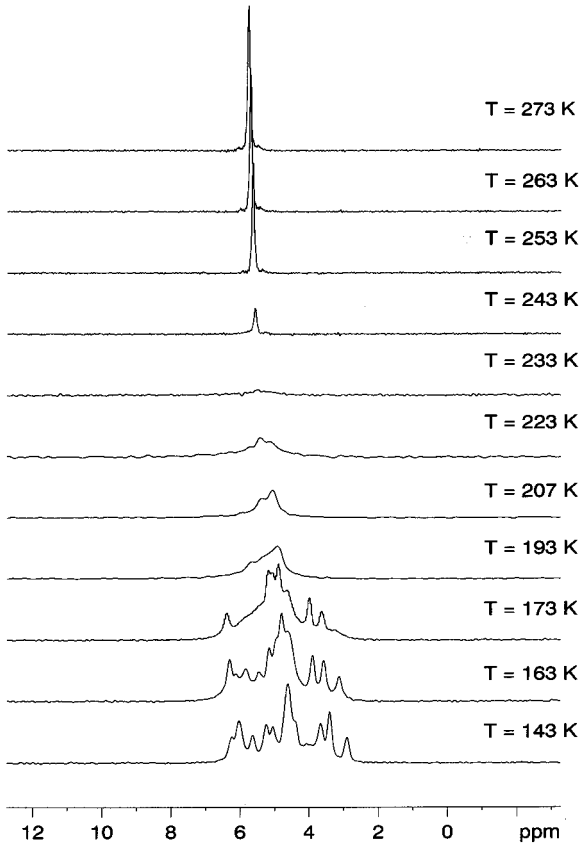

Figure 9. ^{13}C CP/MAS spectra ($\omega_0/2\pi = 75$ MHz) of **2** in the temperature range $T = 143-273$ K.

in low-temperature powder X-ray diffraction measurements of **2**.[12] In the ^{13}C CP/MAS spectra of **2**, the onset of this phase transition is accompanied by a dramatic reduction in CP efficiency. This structural phase transition, and the coexistence of high- and low-temperature phases over a temperature range of ca. $T = 200-235$ K are most easily seen in variable-temperature ^{29}Si CP/MAS spectra of **2** (see Figure 10).

At higher temperatures, one ^{29}Si resonance for all $SiMe_3$ groups and one resonance for the two backbone Si atoms are observed. Below the phase transition temperature, at $T \approx 160$ K, the multiplicity of ^{29}Si resonances is consistent with a complete loss of all molecular symmetry. This, however, has to remain a speculative statement as long as the crystal structure of the low-temperature phase is unknown. Because of the large number of incompletely resolved ^{13}C resonances in the low-temperature phase of **2** (see Figure 9), two-dimensional ^{13}C exchange spectroscopy would be of little help to extract kinetic parameters. Similar arguments apply with respect to ^{29}Si two-dimensional exchange spectroscopy of the low-temperature phase, in addition to problems arising from coexistence of the two phases over a fairly wide temperature range. $Si_2(SiMe_3)_6$ (**2**) is an example where the combination of phase transitions occurring in a temperature range close to the exchange-broadening regime in one-dimensional ^{13}C and ^{29}Si CP/MAS spectra, plus prohibitively high molecular symmetry in the high-temperature phase and very low molecular symmetry in the low-temperature phase, prevents the extraction of meaningful kinetic parameters by means of high-resolution solid-state ^{13}C and ^{29}Si NMR.

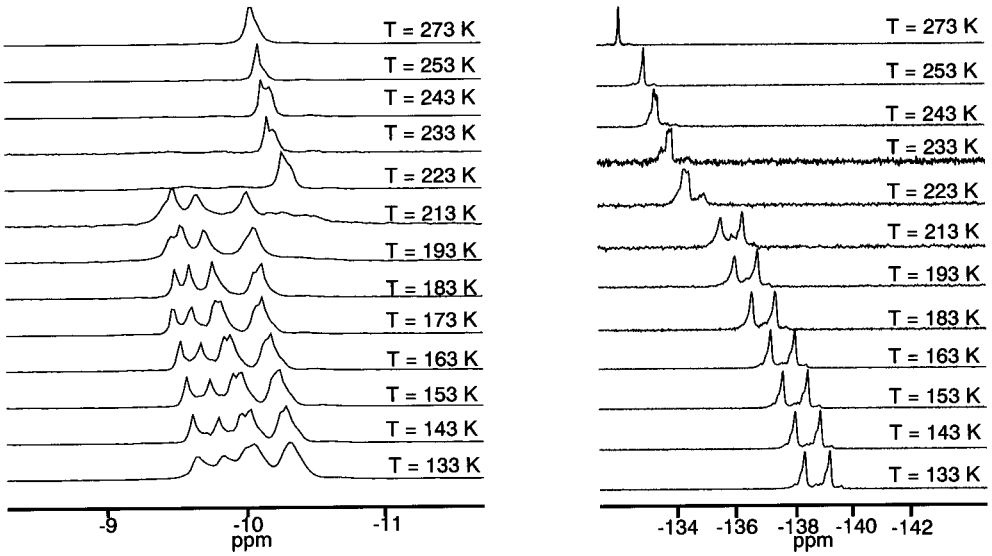

Figure 10. ^{29}Si CP/MAS spectra ($\omega_0/2\pi = 59.6$ MHz) of **2** in the temperature range $T = 133-273$ K. The ^{29}Si resonances shown on the left belong to the $SiMe_3$ groups; the right column depicts the ^{29}Si resonances of the central Si−Si atoms as a function of temperature.

Conclusions

Variable-temperature ^{13}C and ^{29}Si CP/MAS NMR studies of $Si_2{}^tBu_6$ (**1**) and $Si_2(SiMe_3)_6$ (**2**) demonstrate that even the presence of rather extreme *intra*molecular steric crowding does not suppress thermally activated internal reorientational processes in the crystalline solid state. Neglect of the dynamic solid-state properties of crystalline organosilicon compounds may lead to wrong interpretations of ^{13}C and ^{29}Si CP/MAS spectra, obtained under routine conditions at ambient temperatures.

Molecular dynamics calculations, based on geometric information from single-crystal X-ray diffraction studies, are an important complementary tool for NMR studies of dynamic properties of crystalline molecular solids such as **1** and **2**. The extent to which high-resolution solid-state NMR studies are able to provide quantitative information on activation barriers or reorientation rates largely depends on the particular symmetry properties of a given molecule in the crystal structure: cases of intermediate to relatively low molecular point group symmetry (such as **1**) are most informative for in-depth NMR studies. In studies of molecular solids, such as **1** and **2**, where thermally activated reorientational processes *and* structural phase transitions occur as a function of temperature, care needs to be exercised that analysis of reorientational processes is restricted to those temperature regions where there is no interference with the onset of phase-transition-related line shape changes. In unfortunate cases (such as **2**), interference of these two effects may prevent quantitative analysis. In particular, concepts based on inspection of "coalescence regimes" for the extraction of activation parameters from variable-temperature solid-state NMR studies may be dangerously misleading under such circumstances.

Experimental Section

$Si_2{}^tBu_6$ (**1**) was kindly supplied by N. Wiberg, München, Germany, and $Si_2(SiMe_3)_6$ (**2**) by K. Klinkhammer, Stuttgart, Germany. Syntheses of **1**[8] and **2**[9-11] have been described in the literature.

^{13}C CP/MAS experiments have been carried out on Bruker MSL 100, MSL 300, and AM 500 NMR spectrometers, corresponding to ^{13}C Larmor frequencies of 25, 75, and 125 MHz. ^{29}Si CP experiments have only been obtained on the MSL 300 at a ^{29}Si Larmor frequency of 59.6 MHz. Isotropic chemical shifts $\delta(^{13}C)$ and $\delta(^{29}Si)$ are quoted with respect to external $SiMe_4$. MAS frequencies were in the range 1.8−3.5 kHz, cross-polarization contact times were typically between 2 and 5 ms, and recycle delays were between 3 and 6 s; ^{1}H $\pi/2$ pulse durations were in the range 3−5 μs.

Spectral line shape simulations of ^{13}C CP/MAS spectra of **1** were carried out by assuming the superposition of three three-site exchange processes, where the line shape function $g(\omega)$ for a three-site exchange as given by Mehring[16] is

$$g(\omega) = \frac{1}{3}\frac{(\Omega_2 - 27\kappa^2) - i18\kappa(\omega - \langle\omega\rangle)}{2\kappa\Omega_2 + i[\Omega_3 - 9\kappa^2(\omega - \langle\omega\rangle)]} \qquad (3)$$

where κ is the exchange rate constant. Equal integrated intensities for the three subspectra have been assumed in all simulations. For simulation purposes, the experimental spectra have been compensated for the temperature dependence of the isotropic ^{13}C chemical shifts, assuming identical temperature dependencies for all ^{13}C resonances. Preselection of the assignment models within the initial guess of equal internal ^{t}Bu reorientation rates for all three three-site exchanges was performed by a linear least-mean-squares minimization over all experimental spectra in the temperature range $T = 194-230$ K, with the exchange rate constant κ as a single fit parameter. The best models of assignment obtained in this way have been further refined by means of a nonlinear least-mean-squares minimization (MATLAB[17] simplex routine) using the exchange rate constants, line widths, and isotropic chemical shifts of the ^{13}C resonances at 37.9, 37.4, 36.8, 34.2, and 33.8 ppm at $T = 194$ K. Final errors in these fits are defined as the sum of differences of *all* respective, fitted spectra. For none of the fitted spectra over the entire temperature range have any abrupt changes in line widths or chemical shifts as a function of temperature/exchange rate been found.

Molecular dynamics calculations based on the room-temperature single-crystal structure of **1** were performed using

(16) Mehring, M. *Principles of High Resolution NMR in Solids*; Springer: Berlin, 1983.
(17) MATLAB; Math Works Inc., Natick, MA, 1992.

the program Moby (V.1.4),[18] with a 12−6 Lennard−Jones-type potential.[19] The basis set for the calculations was a 30 × 30 × 30 Å cube; all methyl groups were treated as "pseudo-atoms" with a vdW radius of 2 Å (united atom description). Calculations of one-dimensional potential energy profiles were carried out by rotating the respective ^{t}Bu group in 10° steps and by calculating the complete range of orientations around the respective crystallographic equilibrium position.

Acknowledgment. Support of this work by the Deutsche Forschungsgemeinschaft and the Fonds der Chemischen Industrie is gratefully acknowledged. We thank N. Wiberg, München Germany, and K. Klinkhammer, Stuttgart, Germany, for the donation of compounds **1** and **2**, respectively. We wish to thank B. H. Meier, Nijmegen, The Netherlands, for providing generous access to the AM 500 spectrometer, S. Dusold, Bayreuth, Germany, for discussions and for recording 25 MHz variable-temperature ^{13}C CP/MAS spectra of **1**, and X. Helluy, Bayreuth, Germany, for recording static variable-temperature ^{29}Si CP spectra of **1**. We are grateful to A. Simon, Stuttgart, Germany, for low-temperature powder X-ray diffraction measurements on **1** and **2** and for providing the complete data set of the single-crystal X-ray structure determination of **1**, and to M. Veith, Saarbrücken, Germany, for helpful comments concerning the crystal structure of **1**.

OM970120O

(18) Moby V.1.4; Springer New Media; Springer: Berlin, 1991.
(19) Destro, R.; Gavezzotti, A. In *Structure and Properties of Molecular Crystals*; Pierrot, M., Ed.; Studies in Physical and Theoretical Chemistry; Elsevier: Amsterdam, 1990.